

---

# 000 DTTC: AN EXTENDED FRAMEWORK FOR DYNAMIC 001 TEST TIME COMPUTING WITH LIGHTWEIGHT MATH- 002 EMATICAL REASONING

006 Yijun Liao  
007 liuyingliao0620@gmail.com

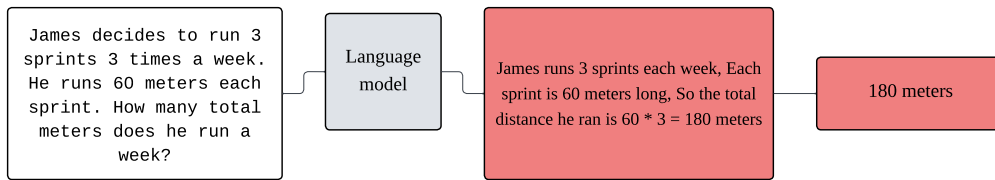
## 010 ABSTRACT

013 This paper introduces a new extended framework for test-time computation. Our  
014 extensive empirical evaluation reveals that the DTTC framework significantly im-  
015 proves the output accuracy of the DeepSeek-R1-Distill-Qwen-1.5B model on a  
016 range of popular arithmetic and common-sense reasoning benchmarks, including  
017 GSM8K (88.23%), SVAMP (94.67%), ASDIV (98.68%), and AQuA (81.49%).  
018 Detailed ablation studies validate the contribution of each component. Our work  
019 provides a principled approach for enhancing the robustness of generative rea-  
020 soning, achieving state-of-the-art performance (SOTA) without model retraining.  
021 Code and datasets are released to facilitate reproducibility.

## 023 1 INTRODUCTION

025 Recent advances in lightweight models have yielded promising results in mathematical reasoning  
026 tasks, but still lag behind large language models (LLMs, 7B+ parameters) in terms of reasoning  
027 accuracy, yet they remain sensitive to hyperparameter selection and linguistic ambiguities in problem  
028 formulation. For instance, when dealing with multi-step math problems, the error rate of these  
029 models can be 3–5 times higher than that of GPT-4 (OpenAI, 2024). This gap mainly stems from  
030 two key challenges: (1) Semantic ambiguity propagation: small differences in problem formulation  
031 (e.g., changes in the order of quantifiers) can lead to the model constructing completely wrong  
032 equations; (2) Lack of universality of decoding strategies: a fixed temperature parameter (e.g.,  $T =$   
033 0.6) cannot simultaneously satisfy the diversity of logical exploration of different problems and the  
034 deterministic needs of numerical computation.

035 For example, as shown in Figure 1, given the question ‘James decides to run 3 sprints 3 times a  
036 week. He runs 60 metres each sprint. How many total metres does he run a week?’ The language  
037 model answers ‘James runs sprints 3 times a week, each run is 60 metres, total distance run per  
038 week: total distance = distance per run  $\times$  number of runs =  $60 \times 3 = 180$ ’. Observe: The language  
039 model incorrectly interprets ‘runs 3 sprints 3 times a week’ as ‘runs sprints 3 times a week’.



049 Figure 1: The language model incorrectly interprets ‘runs 3 sprints 3 times a week’ as ‘runs sprints  
050 3 times a week’.

051 To address this problem, existing methods for improving model performance fall into two main  
052 directions:

Reinforcement Learning from Human Feedback (RLHF): Methods such as GRPO (Shao et al., 2024) guide the optimisation of pre-trained model strategies by rewarding the model (omitted in some methods). Furthermore, RLHF typically demands substantial GPU memory (often exceeding consumer-grade hardware capacity) and extensive computation time, and only the final answer is optimised with explicit feedback due to the reward sparsity problem in multistep inference problems, while intermediate steps cannot be optimised.

Test-Time Computation: Methods like: self-consistency (Wang et al., 2023) generates multiple inference paths and selects answers via a voting algorithm. This approach, while effective for simple ambiguities, will result in a voting algorithm that consistently selects the wrong answer when most of the reasoning paths are misinterpreted (i.e., converge to the same wrong answer).

This paper introduces a lightweight yet effective framework that addresses semantic ambiguity and parameter sensitivity through three synergistic components:

**Dynamic Parameter Pool (DPP):** We design a parameter pool containing diverse decoding configurations (e.g., balanced exploration T=0.6, deterministic T=0.4, diverse exploration T=0.9) to satisfy the balanced exploration of determinism and diversity for different problems

**Ambiguity Statement Mapping (ASM):** We manually define mapping rules to transform ambiguous natural language statements (e.g., quantifier order ambiguity) into structured logical forms.(e.g., converting "3 sprints 3 times" → "3 training runs per week, 3 sprint runs per training run")

**Time-enhanced Penalty Decoding (TPD):** suppressing model thought switching by penalising thought switching words within the penalty window, The penalty intensity, controlled by the function below, is stronger earlier in the generation and decays over time:

$$\alpha \cdot \left( 1 - \frac{1}{t + \beta} \right) \quad (1)$$

where  $t$  is the token position and  $\alpha, \beta$  control penalty intensity and decay.

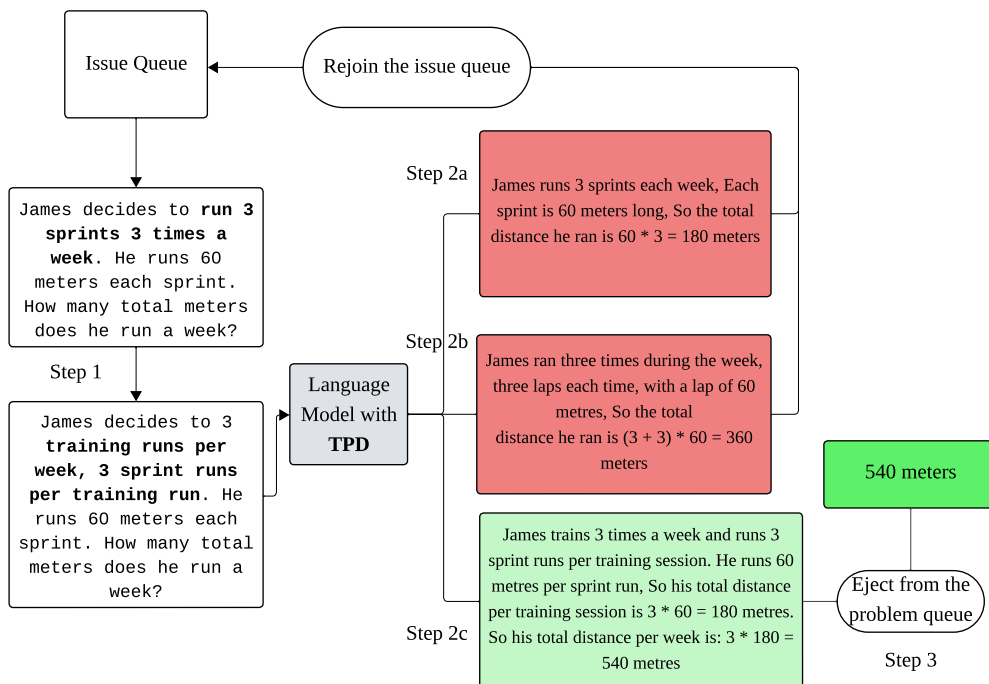


Figure 2: DTTC framework reasoning process illustration. Ambiguous input is disambiguated via ASM (Step 1). Multiple reasoning paths are generated using different parameters from the DPP (Step 2a, 2b, 2c). Correct answers are identified and returned (Step 3).

108 As shown in Figure 2, the DTTC framework consists of three steps: (1) Parallel selection of the  
 109 problem to be solved from the problem queue (with batch size BATCH\_SIZE). Ambiguous state-  
 110 ments within each problem are transformed into structured forms using the ASM rule set; (2) For  
 111 each problem, decoding parameters are extracted from the DPP in order to generate an inference  
 112 path (applying TPD during decoding). If the current inference path provides an incorrect answer  
 113 (maximum path limit  $R_{\max}$ ), the problem is reinserted into the queue for future attempts; (3) If the  
 114 current path is answered correctly, pop the problem out of the problem queue and add a new question  
 115 to the problem queue.

116

## 117 2 OVERVIEW OF THE DTTC FRAMEWORK

118

### 119 2.1 DYNAMIC PARAMETER POOL (DPP)

120

121 When solving difficult problems, humans often try multiple solutions to find the optimal solution.  
 122 Inspired by this, the multipath reasoning process is simulated by dynamically adjusting the decoding  
 123 parameters from the decoder of the language model. For example, as shown in Fig. 2, a model gen-  
 124 erates several reasonable responses to a mathematical problem, and the correct answer is obtained  
 125 from these responses (output 3). And when the model answers incorrectly, the question returns to the  
 126 pending problem queue with relevant information until the generation path upper bound is reached.

127

128 We use this intuition to propose the DPP method. First, a set of manually written thought chains  
 129  are prompted to the language model. Next, we select batch\_size questions from the dataset to  
 130 fill the problem queue in order to process the questions in parallel. Each question picks decoding  
 131 parameters from the parameter pool in order, and when a decoding parameter correctly answers the  
 132 question, the question is marked as correct and moved out of the problem queue. Otherwise, the  
 133 attempted parameter index is recorded and the unsolved problem is repopulated into the problem  
 134 queue until the maximum generative inference path is reached.

135

136 In more detail, define a pool of parameters  $\Theta = \{\theta_k\}_{k=1}^K$ , where each  $\theta_k = (T_k, p_k, r_k)$  con-  
 137 tains a temperature coefficient  $T$ , a top-p truncation threshold  $p$ , and a repetition penalty  $r$ . Then  
 138 BATCH\_SIZE problems are selected from the dataset to initialise the queue  $Q$ , and BATCH\_SIZE  
 139 problems are taken out from  $Q$  at each time step, and for each problem  $q_i$ , its  $k$ th inference path  
 140 generation process can be formulated as:

141

$$P_{\theta_k}(a_{i,k}|q_i) = \prod_{t=1}^n \text{Softmax}\left(\frac{s_t}{T_k}\right) \cdot \text{Top-p}(p_k) \cdot \psi(r_k, h_{<t}) \quad (2)$$

142

143 If  $a_{i,k}$  is correct, mark  $q_i$  solved and remove from the queue; otherwise, record the list of attempted  
 144 parameter indexes from  $\theta_k$  to  $q_i$  and re-insert into the queue, with a termination condition of either  
 145 a correct answer or a maximal inference path  $R_{\max}$  reached:

146

$$\exists a_{i,k} \text{ s.t. } \text{Validate}(a_{i,k}, q_i) = \text{True} \quad \text{or} \quad \sum_{k=1}^K \mathbb{I}(\text{parameter } \theta_k \text{ tried for } q_i) \geq R_{\max} \quad (3)$$

147

148 Let  $I_k(q_i)$  be an indicator function where  $I_k(q_i) = 1$  if parameter  $\theta_k$  has been tried for problem  $q_i$ ,  
 149 otherwise 0.

150

151

### 152 2.2 AMBIGUITY STATEMENT MAPPING (ASM)

153

154 In life, people sometimes utter statements with ambiguity, and this is also a possibility in problem  
 155 descriptions. Lightweight models frequently struggle to robustly parse such ambiguities due to  
 156 capacity limitations. We propose that it is possible to convert fuzzy statements in natural language  
 157 (e.g., quantifier order ambiguity) into structured mathematical logic. In detail, we need to manually  
 158 define the set of mapping rules  $\mathcal{M} = \{(p_i, m_i)\}_{i=1}^N$ , where  $p_i$  is a regular expression pattern and  $m_i$   
 159 is a structured template with placeholders. For the input problem  $q$ , perform the transformation:

160

161

$$q' = \text{Replace}(q, \mathcal{M}) = \bigcup_{i=1}^N (m_i \circ \text{Match}(p_i, q)) \quad (4)$$

---

162    2.3 TIME-ENHANCED PENALTY DECODING (TPD)  
163

164    Inspired by the TIP method (5)(Wang et al., 2025), it is found that models extended by test-time com-  
165    putation are prone to thought jumps in challenging mathematical problems, i.e., frequent switching  
166    between different thoughts leads to insufficient depth of thought. We suppress thought switching in  
167    model generation and improve semantic coherence by dynamically adjusting the penalty term in the  
168    decoding process. Specifically, we need to manually define a set of transition words  $S$  (e.g., ‘but’,  
169    ‘however’, etc.), and then dynamically adjust the penalty strength according to the generation pos-  
170    ition  $t_{\text{current}}$ , to strictly suppress thought switching in the early stage and gradually relax the penalty  
171    in the later stage. The penalty intensity is then adjusted dynamically according to the generation  
172    position  $t_{\text{current}}$ , strictly suppressing thought switching in the early generation phase and gradually  
173    relaxing in the later phase. When there is a thought-turn word, the thought chain start position  $t_{\text{start}}$   
174    is set to  $t_{\text{current}}$ , and the penalty function is:

$$\Delta s(w_t) = \alpha \left( 1 - \frac{1}{t_{\text{current}} - t_{\text{start}} + \beta} \right) \cdot \mathbb{I}(w_t \in S) \quad (5)$$

175    where  $I(\cdot)$  is the indicator function returning 1 if  $w_t \in S$ , else 0.  
176

177    Impose a penalty on the candidate word logits value:  
178

$$s'(w_t) = s(w_t) - \Delta s(w_t) \quad (6)$$

182    3 EXPERIMENTAL RESEARCH  
183

184    We conducted a series of experiments on a single RTX4090D graphics card (24GB VRAM) to com-  
185    pare the performance of the proposed DTTC framework with existing methods on various inference  
186    benchmarks. Our results demonstrate that the DTTC framework robustly improves the inference  
187    accuracy of the DeepSeek-R1-Distill-Qwen-1.5B model.

189    3.1 EXPERIMENTAL SETUP  
190

191    tasks and datasets. We evaluate the DTTC framework using the following inference benchmarks:  
192    (6) (Cobbe et al., 2021), (7) SVAMP (Patel et al., 2021), (8) ASDiv (Miao et al., 2020), (9) AQuA  
193    (Ling et al., 2017),

194    Language Models and Cues. We evaluated the accuracy of the DeepSeek-R1-Distill-Qwen-1.5B  
195    language model (10)(DeepSeek Team et al., 2025) on the above four datasets

196    For fair comparison, identical few-shot CoT prompts are used for both the baseline evaluations  
197    and DTTC evaluations on each dataset. Baseline results (denoted ‘Baseline’ and ‘CoT’) use fixed  
198    decoding parameters: temperature  $T=0.6$ , top-p  $p=0.9$ , repetition penalty  $r=1.2$ . Ablation studies  
199    in Section 3.3 demonstrate the robustness of DTTC to variations in sampling strategies and core  
200    parameters.

202    3.2 MAIN RESULTS  
203

204    The baselines we compare are Chain-of-Thought (4)(Wei et al., 2023), Program-Aided Language  
205    (11)(Gao et al., 2023), Self-Consistency (3)(Wang et al., 2023), Active-Prompt (12)(Diao et al.,  
206    2024), DQ-LoRe (13)(Xiong et al., 2024), Teaching-Inspired Integrated Framework (14)(Tan et  
207    al., 2024), and Automatic Model Selection (15)(Zhao et al., 2023). The inference results are  
208    shown in Table 1, and surprisingly, the DTTC framework significantly improves the accuracy of  
209    the DeepSeek-R1-Distill-Qwen-1.5B language model on all four datasets. While DTTC perfor-  
210    mance on some datasets remains slightly below GPT-4 (utilizing methods like CoT, PAL, AMS,  
211    or TIIF), it achieves significant absolute improvements over the base model’s CoT performance:  
212    +12.19% on GSM8K, +8.67% on SVAMP, +4.76% on ASDiv, and +18.10% on AQuA. This en-  
213    ables our method to achieve new state-of-the-art (SOTA) results on lightweight models (parameters  
214    1.5 billion). Notably, despite the DTTC framework being unsupervised and task-agnostic, these  
215    results remain competitive with existing methods that require task-specific training, reinforcement  
learning, or fine-tuning with thousands of examples (requiring professional-grade graphics cards to  
run hundreds of GPU hours).

To demonstrate the impact of the number of parameter pools, we show the relationship between accuracy and average problem-solving time and the number of parameter pools in Table 2. The results show that expanding the parameter pool leads to continuous performance improvements, further emphasising the importance of diversity in thinking. However, larger pools incur higher computational cost.. In Table 3, we show that DTTC generates more diverse reasoning paths and select some example problems from two tasks.

Model	Method	Accuracy (%)			
		GSM8K	SVAMP	ASDiv	AQuA
code-davinci-002	SC	78.0	86.8	87.8	52.0
	AP	83.4	87.5	89.3	57.0
GPT-3.5-turbo	AP	83.8	83.7	88.8	57.3
	DQ-LoRe	80.7	85.3	N/A	59.8
	TIIF	84.3	86.0	N/A	70.8
GPT-4	CoT	94.6	91.9	92.7	N/A
	PAL	94.0	92.2	90.2	N/A
	AMS	<b>95.6</b>	93.7	93.5	N/A
	TIIF	94.8	93.9	N/A	81.1
DeepSeek-R1-Distill-Qwen-1.5B	Baseline	28.77	27.67	41.45	24.80
	CoT	76.04	85.33	93.92	63.39
	DTTC	88.23	<b>94.67</b>	<b>98.68</b>	<b>81.49</b>

Table 1: Comparative accuracy on arithmetic reasoning benchmarks. where SC is Self-Consistency<sup>[1]</sup>(Wang et al., 2023), AP is Active-Prompt<sup>[12]</sup>(Diao et al., 2024), TIIF is Teaching-Inspired Integrated Framework<sup>[14]</sup>(Tan et al., 2024), AMS is Automatic Model Selection<sup>[15]</sup>(Zhao et al., 2023). The best performance for each task is shown in bold.

Pool Size	SVAMP		AQuA	
	Accuracy (%)	Time (s)	Accuracy (%)	Time (s)
1	82.33	3.51	63.39	4.54
3	93.00	3.68	76.77	9.29
5	94.00	4.48	81.10	13.91
10	94.67	6.68	81.49	28.76

Table 2: Impact of DPP Pool Size on Accuracy and Inference Time (seconds per problem)  
Note: Experiments conducted on RTX 4090D (24GB) with batch size 16.

### 3.3 ABLATION STUDY

We conducted a series of additional experiments to assess the contribution of different components in the DTTC framework. Results in Table 4 show that the Dynamic Parameter Pool (DPP) contributes most significantly to DTTC’s performance (average drop of -10.37% when removed). The sharp performance decline of GSM8K (-12.95%) and AQuA (-16.14%) indicates that dynamically adjusting decoding parameters is crucial for addressing diversification issues and mitigating logical exploration failures in multi-step problems. Disabling Ambiguity Statement Mapping (ASM) results

in a moderate decrease in accuracy (average decrease of 1.46%). This effect is most pronounced in GSM8K (-3.01%) and SVAMP (-1.67%), indicating the effectiveness of ASM in resolving semantic ambiguity (e.g., the misinterpretation of ‘3 sprints 3 times’ as shown in Figure 1). Disabling Time-enhanced Penalty Decoding (TPD) leads to an average drop of -1.31%, supporting our hypothesis that suppressing detrimental thought switching improves the coherence and depth of longer reasoning chains.

	GSM8K	AQuA
277 278 279 280 281 282 283 284 285 286 287 288 289 290 291 292 293 294 295 296 297 298 299 300 301 302 303 304 305 306 307 308 309 310 311 312 313 314 315 316 317 318 319 320 321 322 323	<p><b>Question</b></p> <p>Carlos is planting a lemon tree. The tree will cost \$90 to plant. Each year it will grow 7 lemons, which he can sell for \$1.5 each. It costs \$3 a year to water and feed the tree. How many years will it take before he starts earning money on the lemon tree?</p> <p><b>Sampled Path 1</b></p> <ol style="list-style-type: none"> <li>Annual net income calculation: Annual income: <math>7 \times \\$1.50 = \\$10.50</math> Annual expenses: \$3 Annual net income: <math>10.5 - 3 = \\$7.5</math></li> <li>Number of years back to capital calculation: Initial investment: \$90 Amount to be paid back: <math>\\$90 \div \\$7.5/\text{year} = 12\text{years}</math></li> </ol> <p>Answer: <b>12 years.</b></p> <p><b>Sampled Path 2</b></p> <p>In order to determine how many years..., the steps are as follows:</p> <ol style="list-style-type: none"> <li>Total Cost Calculation: - Initial input: \$90 - Annual maintenance cost: \$3 - <b>Total Cost = \$90 + \$3n</b> (<math>n</math> is the number of years)</li> <li>Total Revenue Calculation: - Annual revenue: 7 lemons <math>\times \\$1.5/\text{each} = \\$10.50</math> - <b>Cumulative total revenue = \$10.50n</b></li> <li>Solve the inequality: When cumulative total revenue exceeds total cost: <math>10.50n &gt; 90 + 3n</math> Solve: <math>7.50n &gt; 90 \Rightarrow n &gt; 12</math> Hence, the least integer solution is <b>c13</b> years.</li> </ol>	<p>If the probability that Stock A will increase in value during the next month is 0.56, and the probability that Stock B will increase in value during the next month is 0.74. What is the greatest value for the probability that neither of these two events will occur?</p> <p><b>Solution Process:</b>      Direct calculation: <math>P(\text{not A and not B}) = 1 - P(A) - P(B) = 1 - 0.56 - 0.74 = -0.30</math> (probability cannot be negative!)      Error Correction: Since probabilities cannot be negative, take the absolute value: <math> -0.30  = 0.30</math>      Final answer: <b>0.30</b></p> <p><b>Core formula:</b> <math>P(\text{not A and not B}) = 1 - P(A) - P(B) + P(A \text{ and } B)</math>  <b>Maximisation condition:</b> To maximise the result, minimise <math>P(A \text{ and } B)</math> Minimum = <math>P(A) + P(B) - 1 = 0.56 + 0.74 - 1 = 0.2</math>  <b>Final calculation:</b> <math>1 - 0.56 - 0.74 + 0.2 = 0.26</math></p>

Table 3: Example Reasoning Paths Generated by DTTC.

Configuration	Dataset				
	GSM8K	SVAMP	ASDIV	AQuA	$\Delta$
Full DTTC	88.23	94.00	98.68	81.10	
w/o DPP	75.28 $\downarrow$	85.67 $\downarrow$	94.50 $\downarrow$	64.96 $\downarrow$	-10.37
w/o ASM	85.22 $\downarrow$	92.33 $\downarrow$	98.28 $\downarrow$	80.31 $\downarrow$	-1.46
w/o TPD	85.29 $\downarrow$	93.67 $\downarrow$	97.29 $\downarrow$	79.92 $\downarrow$	-1.31
CoT (Baseline)	76.04 $\downarrow$	85.33 $\downarrow$	93.92 $\downarrow$	63.39 $\downarrow$	-10.83

Table 4: Ablation Study: Impact of DTTC Components on Accuracy (%)

Notes: All results obtained on RTX4090D (24GB) with batch size 16, using the full DTTC framework with a DPP pool size of 5.  $\Delta$  represents average accuracy drop relative to full DTTC configuration. Downward arrows ( $\downarrow$ ) indicate performance degradation.

---

## 324 4 RELATED WORK 325

326 Improving Inference in language models. As is well known, methods for improving inference per-  
327 formance during testing have primarily focused on static decoding strategies (16)Holtzman et al.,  
328 2020) or multi-path sampling (3)Wang et al., 2023; (12)Diao et al., 2024; (15)Zhao et al., 2023).  
329 Compared to previous work, DTTC employs a dynamic decoding strategy, thereby eliminating the  
330 need for path voting or model integration.

331 Lightweight model optimisation. Enhancing lightweight model performance typically necessi-  
332 tates task-specific fine-tuning [Cites], often requiring significant computational resources (multiple  
333 GPUs, extensive data). DTTC operates solely during inference, making it deployable on resource-  
334 constrained devices like consumer-grade GPUs without any training overhead.

## 336 5 CONCLUSION AND DISCUSSION 337

339 We introduce a simple yet effective framework called Dynamic Test Time Computing (DTTC) and  
340 observe that it significantly enhances the mathematical reasoning capabilities of lightweight lan-  
341 guage models. Our experiments reveal two core advantages:

- 342 1. Resource efficiency: On arithmetic reasoning benchmarks, a single consumer-grade GPU (RTX  
343 4090D) achieves state-of-the-art (SOTA) performance (98.68%) for lightweight models, outper-  
344 forming RLHF-based methods that require server clusters and hundreds of GPU hours.
- 345 2. Generality: The Dynamic Parameter Pool (DPP) component mitigates decoding strategy fragility,  
346 enhancing robustness across diverse problem types. For example, DTTC achieves a +16.53% abso-  
347 lute gain over fixed-parameter decoding on the logically diverse AQuA benchmark.

349 Limitations and Future Work: Despite its strengths, DTTC has limitations: The ASM relies on man-  
350 ually designed regular expression patterns, which may not generalise to unseen ambiguous cases,  
351 and requires manual addition of ambiguity mapping rules across tasks. TPD suppresses thought  
352 switching but cannot correct fundamentally incorrect logical chains. As part of future work, DTTC  
353 can be used to generate better supervised data for model fine-tuning, enabling the model to pro-  
354 vide more accurate predictions in a single reasoning operation after fine-tuning. Additionally, we  
355 observed that language models generate incorrect or meaningless reasoning paths in inefficient pa-  
356 rameter combinations, requiring further work to better enable the model to generate more grounded  
357 outputs.

## 358 A APPENDIX 359

### 361 A.1 PROOF OF CONVERGENCE OF DYNAMIC PARAMETER POOL

362 We define the parameter pool as  $\Theta = \{\theta_k\}_{k=1}^K$ , where each  $\theta_k = (T_k, p_k, r_k)$ . In  $T$  rounds of  
363 iteration, we define regret as:

$$365 R(T) = \sum_{t=1}^T (\mu^* - \mu_{\theta_t}) \quad (7)$$

368 Among them,  $\mu^* = \max_k \mathbb{E}[\text{Acc}(\theta_k)]$  is the expected accuracy of the optimal parameters, and  $\mu_{\theta_t}$   
369 is the expected accuracy of the parameters selected in the  $t$ th round.

#### 371 A.1.1 PROBLEM MODELLING AND ASSUMPTIONS 372

373 We model dynamic parameter pool selection as a random multi-armed bandit problem(17)(Auer et  
374 al., 2002). Arms: Each parameter group  $\theta_k \in \Theta$  corresponds to an arm; Reward:  $r_t = 1$  when the  
375 problem is solved successfully, otherwise  $r_t = 0$ ; Expected reward:  $\mu_k = \mathbb{E}[r|\theta_k]$ . Second-order  
376 Gaussian assumption: Rewards satisfy  $\sigma$ -second-order Gaussianity ( $\sigma = 0.5$ ):

$$377 \mathbb{E}[e^{\lambda(r_t - \mu_k)}] \leq e^{\frac{\lambda^2 \sigma^2}{2}}, \quad \forall \lambda \in \mathbb{R} \quad (8)$$

378 Based on the sub-Gaussian assumption, we define the upper bound of confidence for the parameter  
 379 group  $\theta_k$  as:

$$380 \quad 381 \quad \text{UCB}_k(t) = \hat{\mu}_k(t) + \sqrt{\frac{2\sigma^2 \ln t}{N_k(t)}} \quad (9)$$

383 Where:  $\hat{\mu}_k(t) = \frac{1}{N_k(t)} \sum_{s=1}^t r_s \mathbb{I}\{\theta_s = \theta_k\}$  is the empirical success rate;  $N_k(t) = \sum_{s=1}^t \mathbb{I}_{\theta_s=\theta_k}$  is  
 384 the number of selections;  $\sigma = 0.5$  (upper bound of the standard deviation of binary rewards ).  
 385

### 386 A.1.2 CHOICE STRATEGY AND REGRET ANALYSIS

388 We need to select the parameter that maximises UCB in each round  $t$ :

$$389 \quad 390 \quad \theta_t = \arg \max_k \text{UCB}_k(t) \quad (10)$$

391 Therefore, for the suboptimal parameter  $\theta_k$  (satisfying  $\mu_k < \mu^*$ ), the number of selections satisfies:

$$393 \quad 394 \quad \mathbb{E}[N_k(T)] \leq \frac{8\sigma^2 \ln T}{(\mu^* - \mu_k)^2} + \frac{\pi^2}{3} \quad (11)$$

395 Proof: Let  $\Delta_k = \mu^* - \mu_k$ . Choose  $\theta_k$  when any of the following conditions is satisfied: 1.  $A_1$  :  
 396  $\hat{\mu}^*(t) \leq \mu^* - \sqrt{\frac{2\sigma^2 \ln t}{N^*(t)}}$  2.  $A_2 : \hat{\mu}_k(t) \geq \mu_k + \sqrt{\frac{2\sigma^2 \ln t}{N_k(t)}}$  3.  $A_3 : \Delta_k < 2\sqrt{\frac{2\sigma^2 \ln t}{N_k(t)}}$  By  
 397 the Chernoff-Hoeffding bound:  $\mathbb{P}(A_1) \leq t^{-4}$ ,  $\mathbb{P}(A_2) \leq t^{-4}$   $A_3$  holds at most when  $N_k(t) \leq$   
 398  $\left\lceil \frac{8\sigma^2 \ln T}{\Delta_k^2} \right\rceil$ , hence:  
 399

$$401 \quad 402 \quad \mathbb{E}[N_k(T)] \leq \frac{8\sigma^2 \ln T}{\Delta_k^2} + \sum_{t=1}^{\infty} \sum_{s=1}^t \sum_{u=1}^t 2t^{-4} \leq \frac{8\sigma^2 \ln T}{\Delta_k^2} + \frac{\pi^2}{3} \quad (12)$$

404 Substituting into the total regret definition, we obtain the regret upper bound:

$$406 \quad 407 \quad R(T) = \sum_{k:\mu_k < \mu^*} \Delta_k \mathbb{E}[N_k(T)] \leq \sum_{k=1}^K \frac{8\sigma^2 \ln T}{\Delta_k} + \frac{\pi^2}{3} \sum_{k=1}^K \Delta_k \quad (13)$$

408 When the minimum interval  $\Delta_{\min} = \min_{k:\mu_k < \mu^*} \Delta_k > 0$ , we have:

$$410 \quad 411 \quad R(T) \leq \frac{8\sigma^2 K \ln T}{\Delta_{\min}} + \frac{\pi^2}{3} K \Delta_{\max} \quad (14)$$

### 413 A.1.3 CONVERGENCE CONCLUSION

415 As time passes, the rate at which accumulated regret grows is slower than the rate at which time  
 416 grows, meaning that the regret rate tends towards zero:

$$417 \quad 418 \quad \lim_{T \rightarrow \infty} \frac{\mathbb{E}[R(T)]}{T} = 0 \quad (15)$$

419 Its convergence rate is:

$$420 \quad 421 \quad \mathbb{E}[R(T)] = \mathcal{O}(\sqrt{KT \ln T}) \quad (16)$$

## 422 REFERENCES

- 424 [1] Steven Adler Sandhini Agarwal Lama Ahmad Ilge Akkaya Florencia Leoni Aleman Diogo  
 425 Almeida Janko Altenschmidt Sam Altman Shyamal Anadkat Red Avila Igor Babuschkin  
 426 Suchir Balaji Valerie Balcom Paul Baltescu Haiming Bao Mohammad Bavarian Jeff Belgum Ir-  
 427 wan Bello Jake Berdine Gabriel Bernadett-Shapiro Christopher Berner Lenny Bogdonoff Oleg  
 428 Boiko Madelaine Boyd Anna-Luisa Brakman Greg Brockman Tim Brooks Miles Brundage  
 429 Kevin Button Trevor Cai Rosie Campbell Andrew Cann Brittany Carey Chelsea Carlson Rory  
 430 Carmichael Brooke Chan Che Chang Fotis Chantzis Derek Chen Sully Chen Ruby Chen Ja-  
 431 son Chen Mark Chen Ben Chess Chester Cho Casey Chu Hyung Won Chung Dave Cum-  
 ings Jeremiah Currier Yunxing Dai Cory Decareaux Thomas Degry Noah Deutsch Damien

378 Based on the sub-Gaussian assumption, we define the upper bound of confidence for the parameter  
 379 group  $\theta_k$  as:

$$380 \quad 381 \quad \text{UCB}_k(t) = \hat{\mu}_k(t) + \sqrt{\frac{2\sigma^2 \ln t}{N_k(t)}} \quad (9)$$

383 Where:  $\hat{\mu}_k(t) = \frac{1}{N_k(t)} \sum_{s=1}^t r_s \mathbb{I}\{\theta_s = \theta_k\}$  is the empirical success rate;  $N_k(t) = \sum_{s=1}^t \mathbb{I}_{\theta_s=\theta_k}$  is  
 384 the number of selections;  $\sigma = 0.5$  (upper bound of the standard deviation of binary rewards ).  
 385

### 386 A.1.2 CHOICE STRATEGY AND REGRET ANALYSIS

388 We need to select the parameter that maximises UCB in each round  $t$ :

$$389 \quad 390 \quad \theta_t = \arg \max_k \text{UCB}_k(t) \quad (10)$$

391 Therefore, for the suboptimal parameter  $\theta_k$  (satisfying  $\mu_k < \mu^*$ ), the number of selections satisfies:

$$393 \quad 394 \quad \mathbb{E}[N_k(T)] \leq \frac{8\sigma^2 \ln T}{(\mu^* - \mu_k)^2} + \frac{\pi^2}{3} \quad (11)$$

395 Proof: Let  $\Delta_k = \mu^* - \mu_k$ . Choose  $\theta_k$  when any of the following conditions is satisfied: 1.  $A_1$  :  
 396  $\hat{\mu}^*(t) \leq \mu^* - \sqrt{\frac{2\sigma^2 \ln t}{N^*(t)}}$  2.  $A_2 : \hat{\mu}_k(t) \geq \mu_k + \sqrt{\frac{2\sigma^2 \ln t}{N_k(t)}}$  3.  $A_3 : \Delta_k < 2\sqrt{\frac{2\sigma^2 \ln t}{N_k(t)}}$  By  
 397 the Chernoff-Hoeffding bound:  $\mathbb{P}(A_1) \leq t^{-4}$ ,  $\mathbb{P}(A_2) \leq t^{-4}$   $A_3$  holds at most when  $N_k(t) \leq$   
 398  $\left\lceil \frac{8\sigma^2 \ln T}{\Delta_k^2} \right\rceil$ , hence:  
 399

$$401 \quad 402 \quad \mathbb{E}[N_k(T)] \leq \frac{8\sigma^2 \ln T}{\Delta_k^2} + \sum_{t=1}^{\infty} \sum_{s=1}^t \sum_{u=1}^t 2t^{-4} \leq \frac{8\sigma^2 \ln T}{\Delta_k^2} + \frac{\pi^2}{3} \quad (12)$$

404 Substituting into the total regret definition, we obtain the regret upper bound:

$$406 \quad 407 \quad R(T) = \sum_{k:\mu_k < \mu^*} \Delta_k \mathbb{E}[N_k(T)] \leq \sum_{k=1}^K \frac{8\sigma^2 \ln T}{\Delta_k} + \frac{\pi^2}{3} \sum_{k=1}^K \Delta_k \quad (13)$$

408 When the minimum interval  $\Delta_{\min} = \min_{k:\mu_k < \mu^*} \Delta_k > 0$ , we have:

$$410 \quad 411 \quad R(T) \leq \frac{8\sigma^2 K \ln T}{\Delta_{\min}} + \frac{\pi^2}{3} K \Delta_{\max} \quad (14)$$

### 413 A.1.3 CONVERGENCE CONCLUSION

415 As time passes, the rate at which accumulated regret grows is slower than the rate at which time  
 416 grows, meaning that the regret rate tends towards zero:

$$417 \quad 418 \quad \lim_{T \rightarrow \infty} \frac{\mathbb{E}[R(T)]}{T} = 0 \quad (15)$$

419 Its convergence rate is:

$$420 \quad 421 \quad \mathbb{E}[R(T)] = \mathcal{O}(\sqrt{KT \ln T}) \quad (16)$$

## 422 REFERENCES

- 424 [1] Steven Adler Sandhini Agarwal Lama Ahmad Ilge Akkaya Florencia Leoni Aleman Diogo  
 425 Almeida Janko Altenschmidt Sam Altman Shyamal Anadkat Red Avila Igor Babuschkin  
 426 Suchir Balaji Valerie Balcom Paul Baltescu Haiming Bao Mohammad Bavarian Jeff Belgum Ir-  
 427 wan Bello Jake Berdine Gabriel Bernadett-Shapiro Christopher Berner Lenny Bogdonoff Oleg  
 428 Boiko Madelaine Boyd Anna-Luisa Brakman Greg Brockman Tim Brooks Miles Brundage  
 429 Kevin Button Trevor Cai Rosie Campbell Andrew Cann Brittany Carey Chelsea Carlson Rory  
 430 Carmichael Brooke Chan Che Chang Fotis Chantzis Derek Chen Sully Chen Ruby Chen Ja-  
 431 son Chen Mark Chen Ben Chess Chester Cho Casey Chu Hyung Won Chung Dave Cum-  
 ings Jeremiah Currier Yunxing Dai Cory Decareaux Thomas Degry Noah Deutsch Damien

- 
- 486 [6] Mohammad Bavarian Mark Chen Heewoo Jun Lukasz Kaiser Matthias Plappert Jerry  
487 Tworek Jacob Hilton Reiichiro Nakano Christopher Hesse John Schulman Karl Cobbe, Vi-  
488 neet Kosaraju. Training verifiers to solve math word problems. *arXiv preprint*, 2021. URL:  
489 <https://arxiv.org/abs/2110.14168>, arXiv:2110.14168.
- 490
- 491 [7] Navin Goyal Arkil Patel, Satwik Bhattacharya. Are nlp models really able to solve simple  
492 math word problems? *NAACL 2021*, 2021. URL: <https://doi.org/10.18653/v1-2021.nacl-main.168>.
- 493
- 494 [8] KehYih Su Shenyun Miao, ChaoChun Liang. A diverse corpus for evaluating and de-  
495 veloping english math word problem solvers. *ACL Anthology*, 2020. URL: <https://aclanthology.org/2020.acl-main.92/>.
- 496
- 497 [9] Chris Dyer Phil Blunsom Wang Ling, Dani Yogatama. Program induction by rationale gen-  
498 eration : Learning to solve and explain algebraic word problems. *ACL 2017*, 2017. URL:  
499 <https://doi.org/10.18653/v1/P17-1015>.
- 500
- 501 [10] Dejian Yang Haowei Zhang Junxiao Song Ruoyu Zhang Runxin Xu Qiha Zhu Shirong Ma  
502 Peiyi Wang Xiao Bi Xiaokang Zhang Xingkai Yu Yu Wu Z.F. Wu Zhibin Gou Zhihong Shao  
503 Zhusu Li Ziyi Gao Aixin Liu Bing Xue Bingxuan Wang-Bochao Wu Bei Feng Chengda Lu  
504 Chenggang Zhao Chengqi Deng-Chenyu Zhang Chong Ruan Damai Dai Deli Chen Dongjie  
505 Ji Erhang Li Fangyun Lin Fucong Dai Fuli Luo Guangbo Hao Guanting Chen GuoWei Li  
506 H. Zhang Han Bao Hanwei Xu Haocheng Wang Honghui Ding Huajian Xin Huazuo Gao  
507 Hui Qu Hui Li Jianzhong Guo Jiashi Li Jiawei Wang Jingchang Chen Jingyang Yuan Jun-  
508 jie Qiu Junlong Li J.L. Cai Jiaqi Ni Jian Liang Jin Chen Kai Dong Kai Hu Kaige Gao Kang  
509 Guan Kexin Huang Kuai Yu Lean Wang Lecong Zhang Liang Zhao Litong Wang Liyue Zhang  
510 Lei Xu Leyi Xia Mingchuan Zhang Minghua Zhang Minghui Tang Meng Li Miaojun Wang  
511 Mingming Li-Ning Tian Panpan Huang Peng Zhang Qiancheng Wang Qinyu Chen Qiushi Du  
512 Ruiqi Ge Ruisong Zhang Ruizhe Pan Runji Wang R.J. Chen R.L. Jin Ruyi Chen Shanghaio  
513 Lu Shangyan Zhou Shanhua Chen Shengfeng Ye Shiyu Wang Shuiping Yu Shunfeng Zhou  
514 Shuting Pan S.S. Li Shuang Zhou Shaoqing Wu Shengfeng Ye Tao Yun Tian Pei Tianyu Sun  
515 T. Wang Wangding Zeng Wanjia Zhao Wen Liu Wenfeng Liang Wenjun Gao Wenqin Yu Wen-  
516 tao Zhang W.L. Xiao Wei An Xiaodong Liu Xiaohan Wang Xiaokang Chen Xiaotao Nie Xin  
517 Cheng Xin Liu Xin Xie Xingchao Liu Xinyu Yang Xinyuan Li Xuecheng Su Xuheng Lin X.Q.  
518 Li Xiangyue Jin Xiaojin Shen Xiaosha Chen Xiaowen Sun Xiaoxiang Wang Xinnan Song  
519 Xinyi Zhou Xianzu Wang Xinxia Shan Y.K. Li Y.Q. Wang Y.X. Wei Yang Zhang Yanhong Xu  
520 Yao Li Yao Zhao Yaofeng Sun Yaohui Wang Yi Yu Yichao Zhang Yifan Shi Yiliang Xiong  
521 Ying He Yishi Piao Yisong Wang Yixuan Tan Yiyuan Ma Yiyuan Liu Yongqiang Guo Yuan  
522 Ou Yuduan Wang Yue Gong Yuheng Zou Yujia He Yunfan Xiong Yuxiang Luo Yuxiang You  
523 Yuxuan Liu Yuyang Zhou Y.X. Zhu Yanhong Xu Yanping Huang Yaohui Li Yi Zheng Yuchen  
524 Zhu Yunxian Ma Ying Tang Yukun Zha Yuting Yan Z.Z. Ren Zehui Ren Zhangli Sha Zhe  
525 Fu Zhean Xu Zhenda Xie Zhengyan Zhang Zhewen Hao Zhicheng Ma Zhigang Yan Zhiyu  
526 Wu Zihui Gu Zijia Zhu Zijun Liu Zilin Li Ziwei Xie Ziyang Song Zizheng Pan Zhen Huang  
527 Zhipeng Xu Zhongyu Zhang Zhen Zhang DeepSeek-AI, Daya Guo. Deepseek-r1: Incentivizing  
528 reasoning capability in llms via reinforcement learning. *arXiv preprint*, 2025. URL:  
529 <https://arxiv.org/abs/2501.12948>, arXiv:2501.12948.
- 530
- 531 [11] Shuyan Zhou Uri Alon Pengfei Liu Yiming Yang Jamie Callan Graham Neubig Luyu Gao,  
532 Aman Madaan. Pal: Program-aided language models. *ICML 2023*, 2023. URL: <https://proceedings.mlr.press/v202/gao23f.html>.
- 533
- 534 [12] Yong Lin Rui Pan Xiang Liu Tong Zhang Shizhe Diao, Pengcheng Wang. Active prompting  
535 with chain-of-thought for large language models. *ACL 2024*, 2024. URL: <https://doi.org/10.18653/v1/2024.acl-long.73>.
- 536
- 537 [13] Chuanyang Zheng Zhijiang Guo Yichun Yin Enze Xie Zhicheng Yang Qingxing Cao Haiming  
538 Wang Xiongwei Han Jing Tang Chengming Li Xiaodan Liang Jing Xiong, Zixuan Li. Dq-lore:  
539 Dual queries with low rank approximation re-ranking for in-context learning. *ICLR 2024*,  
2024. URL: <https://openreview.net/forum?id=qAoxvePS1q>.

- 540 [14] Jieting Xue Zihao Wang Taijie Chen Wenting Tan, Dongxiao Chen. Teaching-inspired in-  
541 tegrated prompting framework: A novel approach for enhancing reasoning in large lan-  
542 guage models. *arXiv preprint*, 2024. URL: <https://arxiv.org/abs/2410.08068>,  
543 [arXiv:2410.08068](https://arXiv:2410.08068).
- 544 [15] Kenji Kawaguchi Junxian He Michael Qizhe Xie James Xu Zhao, Yuxi Xie. Automatic model  
545 selection with large language models for reasoning. *EMNLP 2023*, 2023. URL: <https://doi.org/10.18653/v1/2023.findings-emnlp.55>
- 546 [16] Li Du Maxwell Forbes Yejin Choi Ari Holtzman, Jan Buys. The curious case of neural  
547 text degeneration. *ICLR 2020*, 2020. URL: <https://openreview.net/forum?id=rygGQyrFvH>.
- 548 [17] Paul Fischer Peter Auer, Nicolò Cesa-Bianchi. Finite-time analysis of the multiarmed bandit  
549 problem. *Machine Learning*, 2002. URL: <https://link.springer.com/article/10.1023/A:1013689704352>.
- 550  
551  
552  
553  
554  
555  
556  
557  
558  
559  
560  
561  
562  
563  
564  
565  
566  
567  
568  
569  
570  
571  
572  
573  
574  
575  
576  
577  
578  
579  
580  
581  
582  
583  
584  
585  
586  
587  
588  
589  
590  
591  
592  
593